



HAL
open science

A non-invasive implementation of a mixed domain decomposition method for frictional contact problems

Paul Oumaziz, Pierre Gosselet, Pierre-Alain Boucard, Stéphane Guinard

► To cite this version:

Paul Oumaziz, Pierre Gosselet, Pierre-Alain Boucard, Stéphane Guinard. A non-invasive implementation of a mixed domain decomposition method for frictional contact problems. *Computational Mechanics*, 2017, 60, pp.797-812. 10.1007/s00466-017-1444-x . hal-01358379

HAL Id: hal-01358379

<https://hal.science/hal-01358379>

Submitted on 31 Aug 2016

HAL is a multi-disciplinary open access archive for the deposit and dissemination of scientific research documents, whether they are published or not. The documents may come from teaching and research institutions in France or abroad, or from public or private research centers.

L'archive ouverte pluridisciplinaire **HAL**, est destinée au dépôt et à la diffusion de documents scientifiques de niveau recherche, publiés ou non, émanant des établissements d'enseignement et de recherche français ou étrangers, des laboratoires publics ou privés.



Distributed under a Creative Commons Attribution - NonCommercial - ShareAlike 4.0 International License

A non-invasive implementation of a mixed domain decomposition method for frictional contact problems

Paul Oumaziz¹ Pierre Gosselet¹ Pierre-Alain Boucard¹ Stéphane Guinard²

August 31, 2016

Abstract

A non-invasive implementation of the Latin domain decomposition method for frictional contact problems is described. The formulation implies to deal with mixed (Robin) conditions on the faces of the sub-domains, which is not a classical feature of commercial software. Therefore we propose a new implementation of the linear stage of the Latin method with a non-local search direction built as the stiffness of a layer of elements on the interfaces. This choice enables us to implement the method within the opensource software Code_Aster, and to derive 2D and 3D examples with similar performance as standard Latin method.

1 Introduction

Industrialists more and more consider conducting simulation of their products at the scale of the (sub)system instead of the scale of the individual part. To do so, it is crucial to use robust methods capable of handling large contact zones with friction. Such interface law are highly non-regular and complex to handle numerically. The contact formulations often involve Lagrange multipliers [32, 31, 34] and regularization [1, 35]. When the problem can be tracked back to a linear complementary problem, direct solvers, like the Lemke method, are available. However they do not scale efficiently with the number of degrees of freedom. A very general family of iterative methods to handle contact is formed by the Uzawa algorithms [24, 19].

Industrial mechanical simulations also involve large numbers of degrees of freedom. Domain decomposition techniques are suitable to tackle this issue: by distributing the computation over parallel hardware architecture, they lift the memory limits of direct solvers. Moreover when well configured they may accelerate the resolution. Main domain decomposition iterative solvers are: Schwarz methods [17], Balancing Domain Decomposition [27], Finite Element Tearing and Interconnecting [16, 15, 14] as well as their constrained counterparts [8, 13].

However tackling contact within domain decomposition method is not trivial, in particular if one wants the contact interfaces to match the interfaces between sub-domains. One notable adaptation of FETI was proposed in [9, 10, 12, 11]. Robustness of domain decomposition methods was recently significantly improved by the introduction of adapted augmentation spaces obtained through prior quasi-local analysis [33] or multi-preconditioned approaches [21]. However these methods are not yet implemented in commercial software due to their invasive nature and the significant implementation effort required to include them in industrial software.

The Latin method [25] is particularly adapted to treat contact with domain decomposition. In this method, sub-domains and interfaces are considered as different entities with their own mechanical behavior. Under this assumption interfaces behavior corresponds to the nonlinear contact laws. The principle of the method is to separate the linear equations over the sub-domains from the nonlinear local formulation of contact problems, and to formulate the problem as the search of a fixed point. Two successive problems are defined and solved at each iteration: independent linear systems set on sub-domains (linear stage) followed by independent nonlinear pointwise equation on the interfaces with explicit solutions (local stage). The steps of the methods are linked by alternating

¹Paul Oumaziz - Pierre Gosselet - Pierre-Alain Boucard
LMT-Cachan, ENS-Cachan/CNRS/Univ. Paris-Saclay,
61 avenue du président Wilson, 94235 Cachan, FRANCE
Tel.: +33147402402, +33147405333, +33147405330, Fax: +33147402785
oumaziz@lmt.ens-cachan.fr, gosselet@lmt.ens-cachan.fr, boucard@lmt.ens-cachan.fr

²Stéphane Guinard
Computational Structural Mechanics, AGI for Airbus Group Innovations,
18 rue Marius Terce, 31300 Toulouse, FRANCE,
stephane.guinard@airbus.com

directions [18] which can be interpreted as interface stiffnesses (Robin conditions), this connects the Latin method with mixed domain decomposition methods, also known as non-overlapping optimized Schwarz techniques [17].

The current challenge is to implement this method inside a commercial software. The difficulty comes from the treatment of the mixed conditions on the boundary of the sub-domains. Indeed, sub-domains computation with Robin's boundary condition is not a classic feature of commercial mechanical simulation software. Thus we propose a non-invasive approach which enables its implementation. The Robin's condition is dealt with a "non-local" stiffness over the faces of the sub-domains. The search direction is built as a mechanical problem on a layer of elements located on the interfaces. Even though the non-invasive aspect is crucial to the linear stage, this modification implies reformulation of the one from the local stage.

The paper is organized as follow: the reference problem is presented in sub-structured form in section 2. A full description of the non-invasive Latin approach is given in section 3. The contact and friction are treated in section 4. The last section focuses on the numerical studies. A comparison between a "standard" Latin method and the new non-invasive formulation is shown. An 2D academic case is presented to validate the contact computation, then a 3D assembly with frictional contact is treated.

2 Reference problem in substructured form

2.1 Substructured problem

2.1.1 Notations

We consider a family of non-overlapping sub-domains $(\Omega_E)_{E \in [1, N]}$ of \mathbb{R}^d ($d = 1, 2$ or 3). Each sub-domain corresponds to a part of an assembly. We assume each part is constituted by an isotropic linear elastic material whose Hooke's tensor \mathbb{K} is characterized by the Young modulus E and the Poisson ratio ν . Small perturbations and quasi-static isotherm evolutions are assumed. The displacement field is designated by \underline{u} , the stress field by $\boldsymbol{\sigma}$ and the strain field by $\boldsymbol{\varepsilon}$. When needed the subscript E is used for the restriction to sub-domain Ω_E .

Each part Ω_E is subjected to Neumann boundary conditions \underline{F}_d on $\partial_F \Omega_E$, Dirichlet boundary conditions \underline{u}_d on $\partial_u \Omega_E$ and body force \underline{f}_d . It also interacts with any neighboring sub-domain $\Omega_{E'}$ through the interface $\Gamma_{EE'} \subset \partial \Omega_E$. Let \mathcal{E} be the set of all sub-domains and \mathcal{G} the set of all interfaces.

Remarks: Of course we have $\partial \Omega_E \cap \partial \Omega_{E'} \subset \Gamma_{EE'}$, but $\Gamma_{EE'}$ also contains all portions of the boundary which may enter in contact. Thanks to the small displacement hypothesis, this information needs not be updated during the resolution (one piece of the boundary can only interact with one given neighbor).

For each interface, displacement and force fields are defined on the two sides. They are respectively written $(\underline{W}_{EE'}, \underline{W}_{E'E}) \in (H^{1/2}(\Gamma_{EE'}))^2$ and $(\underline{F}_{EE'}, \underline{F}_{E'E}) \in (H^{-1/2}(\Gamma_{EE'}))^2$. $\underline{F}_{EE'}$ represents the force exerted by the sub-domain E' on the sub-domain E . In the case of quasi-static evolution velocity fields $(\dot{\underline{W}}_{EE'}, \dot{\underline{W}}_{E'E})$ are also considered. The interface displacement field is linked to the displacement inside the sub-domain by the trace operator: $\underline{W}_{EE'} = \text{tr}(\underline{u}_E)|_{\Gamma_{EE'}}$.

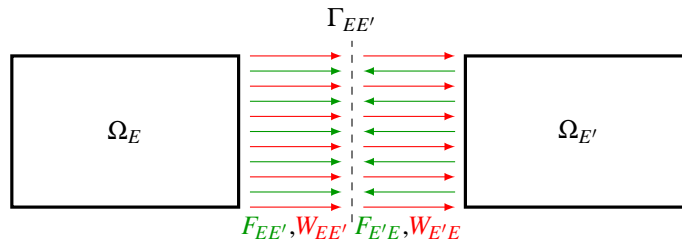


Figure 1: Force and displacement fields of an interface

In our formulation, not only the sub-domains but also the interfaces are granted a mechanical behavior.

2.1.2 Weak formulation on the sub-domains

For any sub-domain Ω_E , let us define local admissibility space $\mathcal{U}_E = \{\underline{u} \in H^1(\Omega_E), \underline{u} = \underline{u}_d \text{ on } \partial_u \Omega_E\}$, and its associated vector space $\mathcal{U}_E^0 = \{\underline{u} \in H^1(\Omega_E), \underline{u} = 0 \text{ on } \partial_u \Omega_E\}$.

The weak formulation can be written as:

$$\forall \Omega_E \in \mathcal{E}, \begin{cases} \forall \dot{\underline{u}}_E \in \mathcal{U}_E^0, \int_{\Omega_E} \underline{\sigma}_E : \varepsilon(\dot{\underline{u}}_E) \, d\Omega = \int_{\Omega_E} \underline{f}_d \cdot \dot{\underline{u}}_E \, d\Omega + \int_{\partial_F \Omega_E} \underline{F}_d \cdot \dot{\underline{u}}_E \, d\Gamma + \sum_{E' \in \Gamma_{EE'}} \int_{\Gamma_{EE'}} \underline{F}_{EE'} \cdot \dot{\underline{u}}_E \, d\Gamma \\ \underline{\sigma}_E = \mathbb{K}_E : \varepsilon(\underline{u}_E) \\ \underline{W}_{EE'} = \text{tr}(\underline{u}_E)|_{\Gamma_{EE'}} \end{cases} \quad (1)$$

where one can recognize the conservation of the momentum of the sub-domain submitted to given loads and neighbors' interactions, the constitutive equation and the trace relation on the interfaces.

2.1.3 Interface behavior

The interface $\Gamma_{EE'}$ can be granted a mechanical behavior given by a relation of the form:

$$\underline{F}_{EE'}(\tau) = b_{EE'} \left(\dot{\underline{W}}_{E'E} - \dot{\underline{W}}_{EE'}, t < \tau \right) \quad (2)$$

Such a relation can be used to model spring interfaces or cohesive interfaces [23, 29]. Note that $b_{E'E}$ is not independent from $b_{EE'}$ because the balance of the interface must be preserved:

$$\underline{F}_{EE'} + \underline{F}_{E'E} = 0 \quad (3)$$

The interface $\Gamma_{EE'}$ can also be granted kinematic constraints, like in the case of perfect cohesion or contact. Typically a perfect interface is characterized by:

$$\begin{cases} \underline{F}_{EE'} + \underline{F}_{E'E} = 0 \\ \underline{W}_{EE'} = \underline{W}_{E'E} \end{cases} \quad (4)$$

Intuitively, perfect and contact interfaces can be considered as limit cases of mechanical behaviors (2) (think of a perfect interface as an infinitely stiff interface). In the following we use the term ‘‘interface behavior’’ and the notation $b_{EE'}$ for any kind of interface, except when being more specific is required.

2.2 Discrete formulation

The continuous formulation above is rather standard in the Latin literature. We now propose to completely describe the resulting discrete system, using operators and notations inspired from [20].

2.2.1 Discretization

A classical FE is used in the sub-domains for the displacement field. Let $\underline{\phi}_E^u$ be the matrix of shape function and \mathbf{U}_E the vector of nodal displacement, such that $\underline{u}_E = \underline{\phi}_E^u \mathbf{U}_E$.

The interface displacement is also discretized with shape functions $\underline{\phi}_{EE'}^w : \underline{W}_{EE'} = \underline{\phi}_{EE'}^w \mathbf{W}_{EE'}$. It is assumed that $\underline{\phi}_{EE'}^w = \underline{\phi}_{E'E}^w$. In the classic description of the Latin method, interface traction ($\underline{F}_{EE'}$) is also discretized. This assumption is not useful in the case of matching grids where the key quantity is the work of the traction in the discretized displacements, that is to say the nodal reactions $\mathbf{F}_{EE'}$:

$$\forall \underline{W}_{EE'}^* = \underline{\phi}_{EE'}^w \mathbf{W}_{EE'}^*, \int_{\Gamma_{EE'}} \underline{F}_{EE'} \cdot \underline{W}_{EE'}^* \, dS = \int_{\Gamma_{EE'}} \underline{F}_{EE'} \cdot (\underline{\phi}_{EE'}^w \mathbf{W}_{EE'}^*) \, dS = \mathbf{W}_{EE'}^{*T} \mathbf{F}_{EE'} \quad (5)$$

In the case where sub-domains have matching grids, we suggest to choose $\underline{\phi}_{EE'}^w = \text{tr}(\underline{\phi}^u)|_{\Gamma_{EE'}}$. In that case we can directly build the discrete counterpart to the trace operator as a boolean matrix $\mathbf{N}_{EE'}$ such that

$$\mathbf{W}_{EE'} = \mathbf{N}_{EE'} \mathbf{U}_E \quad (6)$$

In the case where sub-domains have non-matching grids, sub-domains are connected to the interface by a mortar-like approach [3, 2] which sums up to choosing a discretization for the traction field and ensuring the following work equivalence:

$$\forall \underline{F}_{EE'}^* \in \mathcal{F}_{EE'}(\Gamma_{EE'}), \int_{\Gamma_{EE'}} \underline{F}_{EE'}^* \cdot (\underline{W}_{EE'} - (\text{tr} \underline{u}_E)|_{\Gamma_{EE'}}) \, dS = 0 \quad (7)$$

where the subspace $\mathcal{F}_{EE'}$ is spanned by the shape functions $\underline{\phi}_{EE'}^F$ such that $\int_{\Gamma_{EE'}} \underline{\phi}_{EE'}^F T \underline{\phi}_{EE'}^w$ is invertible. This leads to a non-boolean $\mathbf{N}_{EE'}$ matrix.

To easily handle the many interfaces of one sub-domain, we define concatenated operators:

$$\mathbf{W}_E = \begin{pmatrix} \vdots \\ \mathbf{W}_{EE'} \\ \vdots \end{pmatrix}, \quad \mathbf{F}_E = \begin{pmatrix} \vdots \\ \mathbf{F}_{EE'} \\ \vdots \end{pmatrix}, \quad \mathbf{N}_E = \begin{pmatrix} \ddots & & \\ & \mathbf{N}_{EE'} & \\ & & \ddots \end{pmatrix}, \quad E' \text{ spans all neighbors} \quad (8)$$

In the end, the discrete counterpart to system (1) can be written as:

$$\begin{aligned} \text{Subdomains: } \forall \Omega_E \in \mathcal{E}, & \begin{cases} \mathbf{K}_E \mathbf{U}_E = \mathbf{f}_{dE} + \mathbf{N}_E^T \mathbf{F}_E \\ \mathbf{W}_E = \mathbf{N}_E \mathbf{U}_E \end{cases} \\ \text{Interfaces: } \forall \Gamma_{EE'} \in \mathcal{G}, & \begin{cases} \mathbf{F}_{EE'} + \mathbf{F}_{E'E} = 0 \\ \mathbf{F}_{EE'}(\tau) = \mathbf{b}_{EE'}(\dot{\mathbf{W}}_{E'E} - \dot{\mathbf{W}}_{EE'}, t < \tau) \end{cases} \end{aligned} \quad (9)$$

where \mathbf{f}_{dE} stands for the generalized forces associated to given loads and displacements (it is assumed that non zeros Dirichlet conditions were substituted).

Remarks: The relation between displacement and velocity has not been written to avoid the overloading of the expression. This relation will be implied in the following of the article.

2.2.2 Global notations

Global variables are used to simplify the writing of all the relations. Let's consider a given discrete interface variable $\mathbf{x}_{EE'}$. As said earlier \mathbf{x}_E represents the gathering of all the $(\mathbf{x}_{EE'})_{E'}$. \mathbf{x} will represent the gathering of all the \mathbf{x}_E defined on each sub-domain Ω_E , same procedure applies to operators:

$$\mathbf{x} = \begin{pmatrix} \vdots \\ \mathbf{x}_E \\ \vdots \end{pmatrix}, \quad \mathbf{K} = \begin{pmatrix} \ddots & & 0 \\ & \mathbf{K}_E & \\ 0 & & \ddots \end{pmatrix}, \quad \text{where } E \text{ spans all sub-domains} \quad (10)$$

2.2.3 Sum and difference assembly operator

We introduce operators which permit to make neighboring sub-domains communicate: the operator \mathbf{A} makes sum of interface vectors whereas the operator \mathbf{B} makes differences:

$$\begin{aligned} (\mathbf{A}\mathbf{F})_{|\Gamma_{\{EE'\}}} &= \mathbf{F}_{EE'} + \mathbf{F}_{E'E} \\ (\mathbf{B}\mathbf{W})_{|\Gamma_{\{EE'\}}} &= \mathbf{W}_{E'E} - \mathbf{W}_{EE'} \end{aligned} \quad (11)$$

Because operators \mathbf{A} and \mathbf{B} assemble contributions from neighboring sub-domains, their range lies in an ‘‘in-between interface’’ written $\Gamma_{\{EE'\}}$. There is an arbitrary sign convention in the difference operator which plays no role in the following. Note that because multiple points are handled in the matrix \mathbf{N} , operators \mathbf{A} and \mathbf{B} are full-ranked.

Let $\mathbb{R}^{\{\Gamma\}} = \text{Range}(\mathbf{A}) = \text{Range}(\mathbf{B})$ stands for the vector space supported by the ‘‘in-between interface’’ and $\mathbb{R}^\Gamma = \text{Range}(\mathbf{N})$ be the vector space constituted by the boundary degrees of freedom (on $(\Gamma_{EE'})_{E,E'}$).

The following property is fundamental to handle interface quantities:

Proposition: $\text{Range}(\mathbf{B}^T) \perp \text{Range}(\mathbf{A}^T) = \mathbb{R}^\Gamma$.

When needed, for regular enough interfaces, we will split the normal n and tangential t components.

2.2.4 Discrete problem

Under these notations, the discrete problem equivalent to the sub-structured problem is:

$$\begin{cases} \mathbf{K}\mathbf{U} = \mathbf{f}_d + \mathbf{N}^T \mathbf{F} & \text{Equilibrium of the sub-domains} \\ \mathbf{W} = \mathbf{N}\mathbf{U} & \text{Trace of the sub-domain displacement} \\ \mathbf{F}(\tau) = \mathbf{B}^T \mathbf{b}(\mathbf{B}\dot{\mathbf{W}}, t < \tau) & \text{Interfaces' behavior} \end{cases} \quad (12)$$

This notation for the interface's behavior makes it clear that the equilibrium is ensured: $\mathbf{A}\mathbf{F} = \mathbf{A}\mathbf{B}^T \mathbf{b}(\mathbf{B}\mathbf{W}) = 0$. In the case of perfect interfaces, the equations become:

$$\begin{cases} \mathbf{A}\mathbf{F} = 0 \\ \mathbf{B}\mathbf{W} = 0 \end{cases} \quad (13)$$

Contact is detailed in section 4.

3 The non-invasive quasi-static Latin method

3.1 Principle of the Latin method

3.1.1 Separation of the equations

In order to solve the problem (12), the Latin method [25] is applied. The first idea of the Latin method is to separate the equations in two groups. The first one concerns the sub-domains equations, which in our case are all linear. The second one gathers the equations which manage the behavior of the interfaces, these equations are all local (i.e. pointwise) in space and time.

Remarks: Historically the separation of equations is made between linear and local equations. We will keep this denomination even if sub-domain/interface would be more appropriate in our case.

These two groups define respectively two sets of partial solutions to the problem: \mathcal{A} and \mathcal{L} . The solution of the whole problem is the intersection of these two sets:

$$\mathcal{A} : (\mathbf{F}, \mathbf{W}) \text{ solutions to } \begin{cases} \mathbf{K}\mathbf{U} = \mathbf{f}_d + \mathbf{N}^T \mathbf{F} \\ \mathbf{W} = \mathbf{N}\mathbf{U} \end{cases} \quad (14)$$

$$\mathcal{L} : (\widehat{\mathbf{F}}, \widehat{\mathbf{W}}) \text{ solutions to } \mathbf{F}(\tau) = \mathbf{B}^T \mathbf{b}(\mathbf{B}\dot{\widehat{\mathbf{W}}}, t < \tau) \quad (15)$$

The set \mathcal{A} is an affine space often called space of admissible fields. The set \mathcal{L} is in general a manifold, in the case of perfect interfaces, it is a vector space:

$$\mathcal{L} : (\widehat{\mathbf{F}}, \widehat{\mathbf{W}}) \text{ solutions to } \begin{cases} \mathbf{A}\widehat{\mathbf{F}} = 0 \\ \mathbf{B}\widehat{\mathbf{W}} = 0 \end{cases} \quad (16)$$

3.1.2 Iterations

In order to reach the solution of the whole problem an iterative method is applied where partial solutions are found alternatively in each set \mathcal{A} and \mathcal{L} .

The so-called *local stage* consists in, starting from a partial solution $s_n = (\mathbf{F}_n, \mathbf{W}_n, \dot{\mathbf{W}}_n) \in \mathcal{A}$, searching for a partial solution $\widehat{s}_n = (\widehat{\mathbf{F}}_n, \widehat{\mathbf{W}}_n, \widehat{\dot{\mathbf{W}}}_n) \in \mathcal{L}$. This is made possible by enforcing a search direction of the form:

$$\mathbf{F} - \widehat{\mathbf{F}} - \mathbf{k}_V^+ \left(\dot{\mathbf{W}} - \widehat{\dot{\mathbf{W}}} \right) = 0 \quad (17)$$

where \mathbf{k}_V^+ is an operator which can be chosen by the user. In order to benefit the local character of the equations which define \mathcal{L} , \mathbf{k}_V^+ is often chosen to be diagonal.

The so-called *linear stage* consists in, starting from a partial solution $\widehat{s}_n = (\widehat{\mathbf{F}}_n, \widehat{\mathbf{W}}_n, \widehat{\mathbf{W}}_n) \in \mathcal{L}$, searching for a partial solution $s_{n+1} = (\mathbf{F}_{n+1}, \mathbf{W}_{n+1}, \widehat{\mathbf{W}}_{n+1}) \in \mathcal{A}$. This is made possible by enforcing a search direction of the form:

$$\mathbf{F}_{n+1} - \widehat{\mathbf{F}}_n + \mathbf{k}_V^- (\dot{\mathbf{W}}_{n+1} - \widehat{\mathbf{W}}_n) = 0 \quad (18)$$

where \mathbf{k}_V^- is an operator which can be chosen by the user.

A relaxation is often applied at the end of linear stages:

$$s_{n+1} \leftarrow s_n + \alpha(s_{n+1} - s_n) \quad (19)$$

with $0 < \alpha \leq 1$.

The iterations are graphically represented on Figure 2.

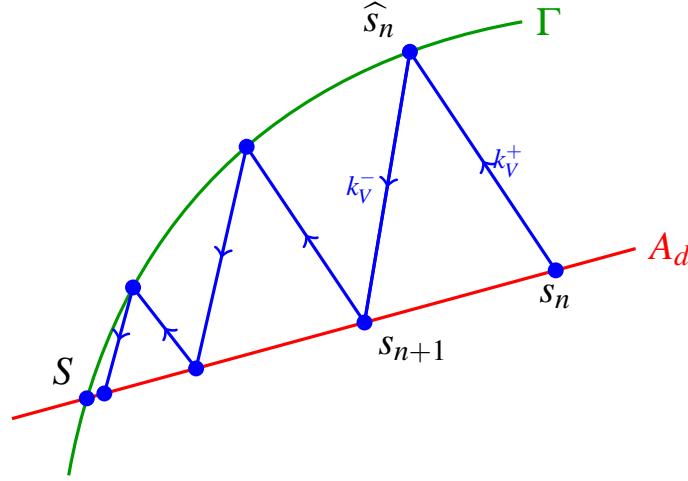


Figure 2: Latin scheme

Proposition: The convergence of the iterations is proved [25] when $\mathbf{k}^- = \mathbf{k}^+$ are symmetric definite positive operator and $\alpha = 0.5$ for maximal monotone behaviours \mathbf{b} .

3.1.3 Interpretation of search directions

Considering an interface $\Gamma_{EE'}$ search directions are often written at the continuous level as a relation of the form:

$$\underline{F}_{EE'} - \widehat{\underline{F}}_{EE'} \pm k_V^{EE'} (\dot{\underline{W}}_{EE'} - \widehat{\underline{W}}_{EE'}) = 0 \quad (20)$$

This leads to the following considerations:

- In its most general meaning, $k_V^{EE'}$ is an operator from $H^{1/2}(\Gamma_{EE'})$ to $H^{-1/2}(\Gamma_{EE'})$. Choosing it to be linear is a classical hypothesis to preserve the linearity of the sub-domains' computations. But it has no reason from being local.
- In the literature, a relation like (20), is often referred to as a generalized Robin condition. A possible way to implement it is to use Ventcell conditions [22].
- In [7] it was proposed to accept the non-locality, and make it clearly appear by choosing a search direction of the following form:

$$J_{EE'}(\underline{F}_{EE'} - \widehat{\underline{F}}_{EE'}) \pm k_V'^{EE'} (\dot{\underline{W}}_{EE'} - \widehat{\underline{W}}_{EE'}) = 0 \quad (21)$$

where $J_{EE'}$ is Riesz isomorphism from $H^{-1/2}(\Gamma_{EE'})$ to $H^{1/2}(\Gamma_{EE'})$, $k_V'^{EE'}$ can easily be chosen to be scalar. This choice leads to dense matrices of search direction which are not computationally tractable.

- In practice, $k_V^{EE'}$ is often taken as a scalar or a local orthotropic operator [30] (without taking the care to use Riesz' isomorphism). In that case the search direction is a classical Robin condition.
- Even when $k_V^{EE'}$ is chosen to be scalar, there remains two possible interpretations of the search direction. First the “weak” interpretation where discretization leads to:

$$\int_{\Gamma_{EE'}} (\underline{\mathbf{F}}_{EE'} - \widehat{\underline{\mathbf{F}}}_{EE'}) \cdot \dot{\mathbf{W}}^* dS \pm \int_{\Gamma_{EE'}} k_V^{EE'} (\underline{\dot{\mathbf{W}}}_{EE'} - \widehat{\underline{\dot{\mathbf{W}}}}_{EE'}) \cdot \dot{\mathbf{W}}^* dS = 0$$

$$\mathbf{F}_{EE'} - \widehat{\mathbf{F}}_{EE'} \pm \mathbf{k}_V^{EE'} (\dot{\mathbf{W}}_{EE'} - \widehat{\dot{\mathbf{W}}}_{EE'}) = 0$$
(22)

and the discrete search direction $\mathbf{k}_V^{EE'}$ is some sort of weighted L^2 -mass matrix of the interface.

Second the “strong” (collocation) interpretation where one directly writes:

$$\mathbf{F}_{EE'} - \widehat{\mathbf{F}}_{EE'} \pm \mathbf{k}_V^{EE'} (\dot{\mathbf{W}}_{EE'} - \widehat{\dot{\mathbf{W}}}_{EE'}) = 0$$
(23)

which has the evident advantage of making the search direction local.

- Note that a local search direction can also be derived from a “weak” interpretation by lumping $\mathbf{k}_{EE'}$ or simply keeping only the diagonal terms.

3.2 The non-invasive Latin method

The mono-scale Latin method is the direct application of the two principles exposed previously. We detail the method in the case of perfect interfaces. The linear stage is presented first since it is mainly impacted by the non-invasive hypothesis. Several possibilities to tackle the local stage are presented afterwards.

3.2.1 Linear stage

The linear stage consists in solving problems on the sub-domains. Equations (14) and (18) lead to the following equations which are independent per sub-domains, and where $(\widehat{\mathbf{F}}, \widehat{\mathbf{W}})$ are known from previous local stage:

$$\text{Solve for } \mathbf{U} \text{ solution to: } \mathbf{K}\mathbf{U} + \mathbf{N}^T \mathbf{k}_V^- \mathbf{N} \dot{\mathbf{U}} = \mathbf{f}_d + \mathbf{N}^T (\widehat{\mathbf{F}} + \mathbf{k}_V^- \widehat{\mathbf{W}})$$
(24)

In order to solve the differential equation on \mathbf{U} , an Euler implicit integration time scheme is applied : $\dot{\mathbf{U}}_{t+1} = \frac{\mathbf{U}_{t+1} - \mathbf{U}_t}{\Delta t}$. That leads to the problem written in displacement:

$$\left(\mathbf{K} + \mathbf{N}^T \frac{\mathbf{k}_V^-}{\Delta t} \mathbf{N} \right) \mathbf{U}_{t+1} = \mathbf{f}_d + \mathbf{N}^T \left(\widehat{\mathbf{F}}^{t+\Delta t} + \mathbf{k}_V^- \widehat{\mathbf{W}}^{t+\Delta t} + \frac{\mathbf{k}_V^-}{\Delta t} \mathbf{W}^t \right)$$
(25)

$$\text{Then compute } \begin{cases} \dot{\mathbf{W}}^{t+\Delta t} = \mathbf{N} \dot{\mathbf{U}}_{t+1} \\ \mathbf{F}^{t+\Delta t} = \widehat{\mathbf{F}}^{t+\Delta t} + \mathbf{k}_V^- \left(\widehat{\mathbf{W}}^{t+\Delta t} - \widehat{\mathbf{W}}^{t+\Delta t} \right) \end{cases}$$
(26)

Remarks: Equation (24) can be interpreted as the discretization of the sub-domains equilibrium under a generalized Robin boundary condition. The term $(\mathbf{N}^T \mathbf{k}_V^- \mathbf{N})$ in (24) corresponds to the interface impedance, it is a non-standard term in commercial software for mechanical problems (there often exist implementations for thermal problems, since it corresponds to convection conditions).

3.2.2 Non-invasive implementation for the linear stage

Here the aim is to propose a new implementation of the generalized Robin condition prone to be implemented in a commercial software. First note that other options were possible:

- first, the interface could be connected to the sub-domain by node-to-node springs elements leading to a local operator.
- second, cohesive elements could be used in their elastic regime. Depending on the chosen quadrature, a local operator can be obtained.

The idea which we investigate in this study, is to think of $\mathbf{k}^- = \mathbf{k}_V^- / \Delta t$ as a generalized Robin condition which can be realized by adding matter on the boundary of the sub-domains. This strategy leads to a non-local search direction.

The matter added at interface $\Gamma_{EE'}$ is written $\theta_{EE'}$, the Hooke tensor associated to its behavior is $\mathbb{K}_{\theta_{EE'}}$. The addition is called a sole. A zero Dirichlet condition is imposed on the part $\partial_u \mathbb{K}_{\theta_{EE'}}$ of the boundary of the sole which is not in contact with the interface.

At the continuous level, the search direction operator written in displacement $\underline{k}_{EE'}$ is defined by the following relation:

$$\underline{F}_{EE'} = k_{EE'}(\underline{W}_{EE'}) \quad \Leftrightarrow \quad \begin{cases} \underline{u} \in H^1(\theta_{EE'}), \underline{u} = \underline{W}_{EE'} \text{ on } \Gamma_{EE'}, \underline{u} = 0 \text{ on } \partial_u \theta_{EE'} \\ \forall \underline{v} \in H^1(\theta_{EE'}), \underline{v} = 0 \text{ on } \Gamma_{EE'} \cup \partial_u \theta_{EE'} \\ \int_{\theta_{EE'}} \varepsilon(\underline{v}) : \mathbb{K}_{\theta_{EE'}} : \varepsilon(\underline{u}) \, d\Omega = \int_{\Gamma_{EE'}} \underline{F}_{EE'} \cdot \underline{v} \, dS \end{cases} \quad (27)$$

At the discrete level, if $\mathbf{K}_{\theta_{EE'}}$ is the stiffness matrix of the sole (with zero Dirichlet boundary conditions taken into account), then \mathbf{k}^- is the Schur complement of $\mathbf{K}_{\theta_{EE'}}$ which condenses the stiffness on the interface degrees of freedom.

Remarks: A parallel can be done with the Restricted Additive Schwarz method [4, 5]. Indeed the matter addition at the interface may be seen as an overlap between two sub-domains. However contrary to the Schwarz method, the boundary of the overlap which is not in contact with the interface is blocked, whereas a displacement come from the sub-domains is imposed in the Schwarz method. Moreover the material characteristics of the added matter is a parameter of the method.

From an implementation point of view, solving the problem of the linear stage $(\mathbf{K} + \mathbf{N}^T \mathbf{k}^- \mathbf{N})$ corresponds to solving a mechanical problem on the sub-domain extended with the sole, loaded by an inner interface traction field, (Figure 3) which is a classic operation in most software. This permits to compute $\mathbf{W}_{EE'}$ and \mathbf{U}_E .

The nodal reaction $\mathbf{F}_{EE'}$ can be obtained by post-processing the sub-domain or by computing a Dirichlet problem on the sole alone.

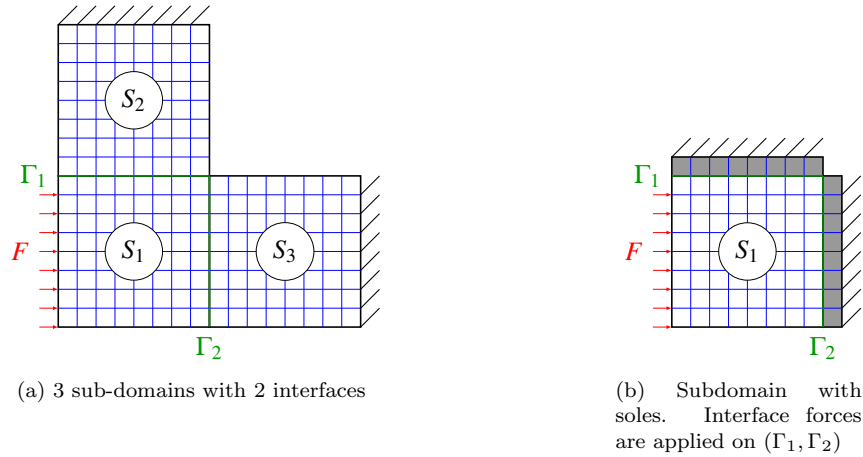


Figure 3: Example of a problem to solve at linear stage

Remarks:

- The indicator is post-processed from the linear stage.
- The indicator depends on the search direction.
- Other indicators based on true errors \mathbf{AF} and \mathbf{BW} , which are computed at the begin of the local step can also be used.

4 Treatment of the contact

4.1 Frictionless contact

In order to write the contact problem, we assume sufficient smoothness for the interface so that we can define a local basis at each interface node: n stands for the outer normal direction and t for the tangent direction (the tangent basis is (t_1, t_2) in 3D). Conventionally the same normal vector is used on both neighbors, the orientation of the vector is chosen in agreement with the sign convention of \mathbf{B} . Thus we assume all vectors and matrix are turned in the local interface frame (n, t) .

In order to preserve locality, the search direction must be a diagonal operator (in the normal-tangent frame). Note that obtaining such an operator is not trivial in the case of search directions obtained with matter addition. In our case the diagonal of the stiffness operator of the sole is chosen.

The local stage for contact interfaces regroups the different relations that govern the contact plus the search directions written in term of velocity. As for the linear stage, an implicit scheme is applied to link the speed distribution and the displacement distribution. Thus the problem to solve becomes:

$$\text{Find } \left(\widehat{\mathbf{W}}^{t+\Delta t}, \widehat{\dot{\mathbf{W}}}^{t+\Delta t}, \widehat{\mathbf{F}}^{t+\Delta t} \right) \text{ solution to: } \begin{cases} \mathbf{B}_n \widehat{\mathbf{W}}_n^{t+\Delta t} + \mathbf{j}_n \geq 0 \\ \mathbf{A} \widehat{\mathbf{F}}^{t+\Delta t} = 0 \\ \mathbf{B}_n \widehat{\mathbf{F}}_n^{t+\Delta t} \geq 0 \\ \mathbf{B}_t \widehat{\mathbf{F}}_t^{t+\Delta t} = 0 \\ \left(\mathbf{B}_n \widehat{\mathbf{F}}_n^{t+\Delta t} \right)^T \left(\mathbf{B}_n \widehat{\mathbf{W}}_n^{t+\Delta t} + \mathbf{j}_n \right) = 0 \\ \widehat{\mathbf{F}}^{t+\Delta t} - \mathbf{F}^{t+\Delta t} - \mathbf{k}_V^+ \left(\widehat{\dot{\mathbf{W}}}^{t+\Delta t} - \dot{\mathbf{W}}^{t+\Delta t} \right) = 0 \\ \widehat{\mathbf{W}}^{t+\Delta t} = \widehat{\mathbf{W}}^t + \Delta t \widehat{\dot{\mathbf{W}}}^{t+\Delta t} \end{cases} \quad (34)$$

where hat-less quantities and quantities at time step t are known from previous time step and linear stage. \mathbf{j}_n is the initial normal gap.

To solve the problem, the time integration scheme is used in the non-interpenetration relation, and then the search direction is applied to make $\widehat{\mathbf{F}}^{t+\Delta t}$ appear, so that we can control the sign of the normal component.

$$\mathbf{B}_n \widehat{\mathbf{W}}_n^{t+\Delta t} + \mathbf{j}_n = \mathbf{B}_n \widehat{\mathbf{W}}_n^t + \mathbf{j}_n + \Delta t \mathbf{B}_n \left(\dot{\mathbf{W}}_n^{t+\Delta t} + \mathbf{k}_{V_n}^+{}^{-1} \left(\widehat{\mathbf{F}}_n^{t+\Delta t} - \mathbf{F}_n^{t+\Delta t} \right) \right) \geq 0 \quad (35)$$

which can be reorganized as:

$$\underbrace{\mathbf{B}_n \widehat{\mathbf{W}}_n^t + \mathbf{j}_n + \Delta t \mathbf{B}_n \dot{\mathbf{W}}_n^{t+\Delta t} - \Delta t \mathbf{B}_n \mathbf{k}_{V_n}^+{}^{-1} \mathbf{F}_n^{t+\Delta t}}_{\mathbf{C}_n} + \Delta t \mathbf{B}_n \mathbf{k}_{V_n}^+{}^{-1} \widehat{\mathbf{F}}_n^{t+\Delta t} \geq 0 \quad (36)$$

\mathbf{C}_n is a computable quantity which enables us to evaluate nodewise the feasibility of a contactless solution. In the following non-bold characters stand for a given node, we have:

$$\boxed{\begin{cases} \text{Contact} & \Leftrightarrow C_n \leq 0 \\ \text{No-contact} & \Leftrightarrow C_n > 0 \end{cases}} \quad (37)$$

No contact case $\boxed{C_n > 0}$

In that case, the solution $\widehat{\mathbf{F}}_n^{t+\Delta t} = 0$ and $\mathbf{B}_n \widehat{\mathbf{W}}_n^{t+\Delta t} + \mathbf{j}_n = C_n > 0$ satisfies all equations.

Contact case $C_n \leq 0$

In that case, the solution is $\Delta t B_n k_{V_n}^+{}^{-1} \widehat{F}_n^{t+\Delta t} = -C_n \geq 0$ and $B_n \widehat{W}_n^{t+\Delta t} + j_n = 0$. To compute $\widehat{F}_n^{t+\Delta t}$ one simply has to remember that it can be expressed as $\widehat{F}_n^{t+\Delta t} = B_n^T F_n^*$ for some F_n^* (indeed $\widehat{F}_n^{t+\Delta t}$ verifies $A_n \widehat{F}_n^{t+\Delta t} = 0$), and thus:

$$\boxed{F_n^{t+\Delta t} = -B_n^T \left(B_n k_{V_n}^+{}^{-1} B_n^T \right)^{-1} \frac{C_n}{\Delta t}} \quad (38)$$

$\widehat{W}_n^{t+\Delta t}$ then can be deduced using the search direction and the time integration.

For the tangential component of the interface distributions, we use the fact that $\widehat{F}_t^{t+\Delta t} = 0$. Then with the search direction and the temporal integration scheme, we obtain :

$$\boxed{\begin{aligned} \widehat{W}_t^{t+\Delta t} &= \dot{W}_t^{t+\Delta t} - k_{V_t}^+{}^{-1} F_t^{t+\Delta t} \\ \widehat{W}_t^{t+\Delta t} &= \widehat{W}_t^{t+\Delta t} + \Delta t \left(\dot{W}_t^{t+\Delta t} - k_{V_t}^+{}^{-1} F_t^{t+\Delta t} \right) \end{aligned}} \quad (39)$$

As a conclusion it is possible to define a nodewise indicator which gives the contact status. This indicator can be expressed only with the distribution $(\widehat{W}_t, \dot{W}_t^{t+\Delta t}, F_t^{t+\Delta t})$ known from the previous linear stage and previous time step of local stage. Then the computation of the solutions $(\widehat{W}^{t+\Delta t}, \widehat{W}^{t+\Delta t}, \widehat{F}^{t+\Delta t})$ is explicit.

4.2 Coulomb friction

The frictional aspect is taken into account by adding new conditions in the case of contact. First the normal components can be found as explained in previous subsection. Then in the case of contact, another indicator is computed to evaluate the possibility of sliding.

Let μ be Coulomb's friction coefficient. The friction conditions can be written nodewise as:

$$\left\{ \begin{array}{l} \text{If } \|\widehat{F}_t^{t+\Delta t}\| \leq \mu |\widehat{F}_n^{t+\Delta t}| \text{ then } B_t \widehat{W}_t^{t+\Delta t} = 0 \\ \text{If } \|\widehat{F}_t^{t+\Delta t}\| = \mu |\widehat{F}_n^{t+\Delta t}| \text{ then } \exists \lambda > 0, B_t \widehat{W}_t^{t+\Delta t} = \lambda (B_t B_t^T)^{-1} B_t \widehat{F}_t^{t+\Delta t} \end{array} \right. \quad (40)$$

where $\widehat{F}_t^{t+\Delta t}$ is still submitted to the balance condition $A_t \widehat{F}_t^{t+\Delta t} = 0$.

With the same idea as for frictionless contact, it is possible to define an indicator that makes precise the status of the node. The tangential component of the force distribution is computed and compared to the norm of the normal one. Beforehand, as the search direction is semi positive definite, a decomposition of the tangential velocity distribution is done:

$$\exists (\alpha, \beta), \widehat{W}_t^{t+\Delta t} = A_t^T \alpha + k_{V_t}^+{}^{-1} B_t^T \beta \quad (41)$$

$A_t^T \alpha$ corresponds to the sticking part whereas $k_{V_t}^+{}^{-1} B_t^T \beta$ corresponds to the sliding part.

With such an expression for the velocity distribution, the search direction is used to computed the force distribution:

$$\widehat{F}_t^{t+\Delta t} = F_t^{t+\Delta t} + k_{V_t}^+ \left(\widehat{W}_t^{t+\Delta t} - \dot{W}_t^{t+\Delta t} \right) \quad (42)$$

Applying the equilibrium of the force distribution, α can be determined as:

$$\alpha = (A_t k_{V_t}^+ A_t^T)^{-1} A_t \left[k_{V_t}^+ \dot{W}_t^{t+\Delta t} - F_t^{t+\Delta t} \right] \quad (43)$$

Thus the expression of the force distribution becomes:

$$\widehat{F}_t^{t+\Delta t} = \underbrace{\left[\mathbb{I} - k_{V_t}^+ A_t^T (A_t k_{V_t}^+ A_t^T)^{-1} A_t \right] F_t^{t+\Delta t} - k_{V_t}^+ \left[\mathbb{I} - A_t^T (A_t k_{V_t}^+ A_t^T)^{-1} A_t k_{V_t}^+ \right] \dot{W}_t^{t+\Delta t} + B_t^T \beta}_{G_t} \quad (44)$$

G_t represents the sticking contribution to the force distribution. It only depends on contributions from the linear stage and so can be computed directly at the local stage. It is used as a nodewise indicator for the possibility of sliding.

$$\begin{array}{l} \text{Sticking} \quad \Leftrightarrow \|G_t\| \leq \mu|F_n^{t+\Delta t}| \\ \text{Sliding} \quad \Leftrightarrow \|G_t\| > \mu|F_n^{t+\Delta t}| \end{array} \quad (45)$$

Sticking case If $\|G_t\| \leq \mu|\widehat{F}_n^{t+\Delta t}|$

We can directly set $\beta = 0$, $\widehat{F}_t^{t+\Delta t} = G_t$. The velocity distribution is computed with the expression of α .

$$\begin{cases} \widehat{W}_t^{t+\Delta t} = A_t^T (A_t k_{V_t}^+ A_t^T)^{-1} A_t (k_t^+ \dot{W}_t^{t+\Delta t} - F_t^{t+\Delta t}) \\ \widehat{W}_t^{t+\Delta t} = \widehat{W}_t^t + \Delta t \widehat{W}_t^{t+\Delta t} \end{cases} \quad (46)$$

Sliding case: If $\|G_t\| > \mu|\widehat{F}_n^{t+\Delta t}|$

β and $\lambda > 0$ must be found such that $\|\widehat{F}_t^{t+\Delta t}\| = \mu|\widehat{F}_n^{t+\Delta t}|$ and $B_t \widehat{W}_t^{t+\Delta t} = \lambda (B_t B_t^T)^{-1} B_t \widehat{F}_t^{t+\Delta t}$.

With the expression of the tangential component of the velocity, the traction can be expressed as a function of β and λ :

$$(B_t B_t^T)^{-1} B_t \widehat{F}_t^{t+\Delta t} = \frac{1}{\lambda} B_t k_{V_t}^+{}^{-1} B_t^T \beta \quad (47)$$

Moreover $\widehat{F}_t^{t+\Delta t} = G_t + B_t^T \beta$. Thus the relation between β and λ is:

$$(B_t B_t^T)^{-1} B_t G_t + \beta = B_t k_{V_t}^+{}^{-1} B_t^T \frac{\beta}{\lambda} \quad (48)$$

and

$$\beta = \lambda \left(-\lambda \mathbb{I} + B_t k_{V_t}^+{}^{-1} B_t^T \right)^{-1} (B_t B_t^T)^{-1} B_t G_t \quad (49)$$

The tangential force distribution can be expressed as a function of λ :

$$\widehat{F}_t^{t+\Delta t} = \left(\mathbb{I} - B_t^T \left(\mathbb{I} - \frac{B_t k_{V_t}^+{}^{-1} B_t^T}{\lambda} \right)^{-1} (B_t B_t^T)^{-1} B_t \right) G_t \quad (50)$$

And $\lambda > 0$ is determined by the relation $\|\widehat{F}_t^{t+\Delta t}\| = \mu|\widehat{F}_n^{t+\Delta t}|$ given from the sliding assumption. It is more convenient to consider the intermediate quantity (non-redundant between the two sides of the interface): $\|(B_t B_t^T)^{-1} B_t \widehat{F}_t^{t+\Delta t}\| = \mu|(B_n B_n^T)^{-1} B_n \widehat{F}_n^{t+\Delta t}|$. Then we must ensure:

$$\left\| \left(\mathbb{I} - \left(\mathbb{I} - \frac{B_t k_{V_t}^+{}^{-1} B_t^T}{\lambda} \right)^{-1} \right) \underbrace{(B_t B_t^T)^{-1} B_t G_t}_{G'_t} \right\| = \underbrace{\mu|(B_n B_n^T)^{-1} B_n \widehat{F}_n^{t+\Delta t}|}_D \quad (51)$$

Note that the square matrices are all diagonal.

Remarks:

- $\widehat{F}_t^{t+\Delta t}$ can be expressed as $\widehat{F}_t^{t+\Delta t} = \underline{\underline{\gamma}} G'_t$ as $\underline{\underline{\gamma}} = \left(\mathbb{I} - \left(\mathbb{I} - \frac{B_t k_{V_t}^+{}^{-1} B_t^T}{\lambda} \right)^{-1} \right)$
- In a 2D case, $\underline{\underline{\gamma}} \in \mathbb{R}_+^*$ and $G'_t \in \mathbb{R}$ so the unknown γ is easily computed with $\gamma = \frac{\mu|\widehat{F}_n^{t+\Delta t}|}{\|G'_t\|}$ and therefore:

$$\widehat{F}_t^{t+\Delta t} = \mu|\widehat{F}_n^{t+\Delta t}| \frac{G'_t}{\|G'_t\|} \quad (52)$$

- In a general 3D case, the equation 51 is a polynomial equation of the forth degree. However, in the case of the two tangential search directions are equal, $\underline{\underline{\gamma}} = \gamma \mathbb{I}$ with $\gamma > 0$. Under this assumption, a similar result than previously is obtained: $\gamma = \frac{\mu |\widehat{F}_n^{t+\Delta t}|}{\|G'_t\|}$ and therefore:

$$\boxed{\widehat{F}_t^{t+\Delta t} = \mu |\widehat{F}_n^{t+\Delta t}| \frac{G'_t}{\|G'_t\|}} \quad (53)$$

- The velocity distribution $\widehat{W}^{t+\Delta t}$ is computed with the relation of the search direction and the expression of the force distribution $\widehat{F}^{t+\Delta t}$. Then the displacement is computed with the temporal integration scheme.

The Latin method for frictional contact is summarized in algorithm 1.

Algorithm 1: Summary of the Latin method

Input: Initialisation

while *Error criterion* < *objective* **do**

Local stage:

foreach *time step* **do**

foreach *interface* **do**

if *interface is perfect* **then**

 Non-local computation on a double sole to obtain displacement : $\mathbf{W}^{t+\Delta t}$

 Explicit time scheme to compute velocity : $\widehat{\mathbf{W}}^{t+\Delta t}$

 Search direction to compute force : $\widehat{\mathbf{F}}^{t+\Delta t}$

else

 Contact interface:

for *each node on the interface* **do**

 Compute the contact indicator C_n

if $C_n \geq 0$ **then**

 | No contact computation

else

 Contact computation

 Compute the sticking indicator G_t

if $\|G_t\| \leq \mu |\widehat{F}_n^{t+\Delta t}|$ **then**

 | Sticking computation

else

 | Sliding computation

end

end

end

end

end

end

Linear stage:

foreach *time step* **do**

foreach *sub-domain* **do**

 Computation of displacement $\mathbf{W}^{t+\Delta t}$ by solving a problem on sub-domain plus soles

 Explicit time scheme to compute velocity : $\widehat{\mathbf{W}}^{t+\Delta t}$

 Search direction to compute force : $\widehat{\mathbf{F}}^{t+\Delta t}$

 Relaxation step: $s_{n+1} \leftarrow s_n + \alpha(s_{n+1} - s_n)$;

end

end

end

5 Numerical examples

First a validation of implementation of the non-invasive aspect is presented in 5.1 compared to a “standard” Latin with an invasive modification of the stiffness operator. This validation is performed on a simple traction beam study. Moreover the influence of the search direction on the convergence is shown. An academical test case for contact with friction is presented in 5.2. The objective is to validate the frictional contact by comparing results with the ones in [6]. A 3D study of a bolted assembly involving frictional contact with initial gap and pre-load interfaces is developed in 5.3. The computations are made with Code_Aster driven by a python instance.

5.1 Comparison ”standard Latin” / non-invasive Latin

The comparison between a “standard” invasive Latin method and the non-invasive one is performed on a simple traction beam problem fixed on one side and under a load F on the other side (Figure 4). The Young modulus is E , the length L and a section S . A sub-structuring in 5 sub-domains is chosen. In this 1D case, the search direction is reduced to only one parameter per interface.

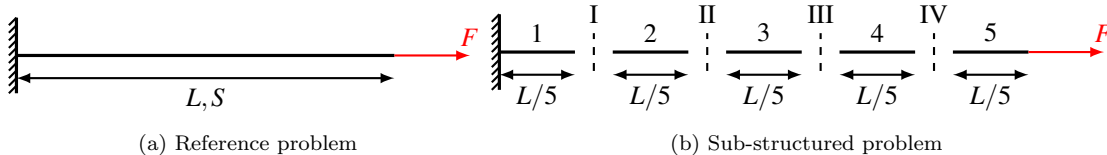


Figure 4: Traction beam

For the standard computation $\mathbf{k}^- = \mathbf{k}^+ = \frac{ES}{L}$ [25]. For the non-invasive version, the parameter is reduced to the Young modulus of the soles and therefore it is easy to obtain equivalent search directions for the two cases by choosing E_s the Young modulus of the soles as $E_s = E \frac{L_s}{L}$ with L_s the length of the soles. As the soles are composed with a layer of one element, the size L_s is equal to the discretization h . A parametric computation is led to study the impact of the search direction on the convergence.

The numerical value of the parameters are given on the Table 1.

Parameters	Value
E	200 GPa
L	100 mm
S	10 mm
$h=L_s$	1 mm

As seen on the Figure 5 the standard and the non-invasive Latin method give the same results. This validates the non-invasive implementation.

On figure 6 the parametric study is presented to illustrate the dependency of convergence on the search direction. We use the multiplicative parameter α as $\mathbf{k}^- = \mathbf{k}^+ = \alpha \frac{ES}{L}$ for several sub-structuring. The dimensions of the global structure and the size of the discretization are the same for all the sub-structuring case. The results show that an optimal search direction exists and that it does not depend on the choice of the sub-structuring. The optimal search direction depends on the global structure. These two results are classical for the Latin computation.

Actually as the optimal search direction is not evident to compute for any structure, we keep a “non-optimal” standard one but sufficient to reach good level of convergence (indicator $< 10^{-5}$). The rule to choose $\mathbf{k}^+ = \mathbf{k}^- = \frac{ES}{L}$ is chosen. For 2D or 3D structure that is translated by adjusting the Young modulus of the soles to ensure that soles and sub-domains have approximatively the same rigidity.

5.2 An academic 2D friction case

the developed contact management is exemplified on an academic use-case [6]. The quasi-static problem is presented on the Figure 7. Two interfaces with frictional contact link respectively the sub-domains (1,2) and the sub-domains (2,3) with the parameters μ_1 and μ_2 as Coulomb coefficients. An additional interface enables to manage a boundary

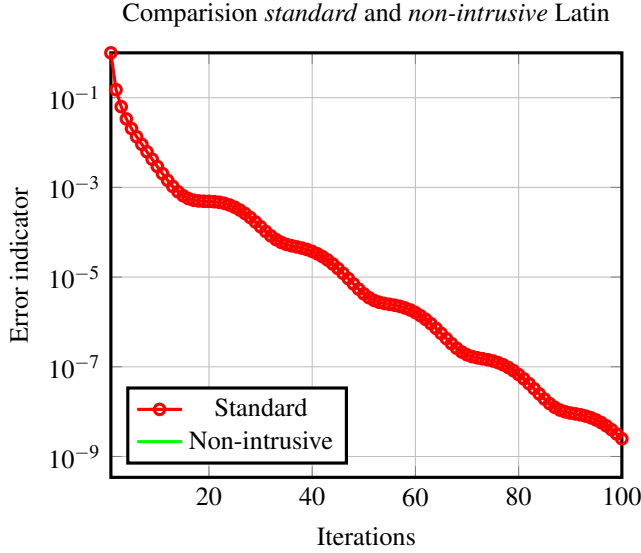


Figure 5: Comparison between the standard and the non-intrusive Latin

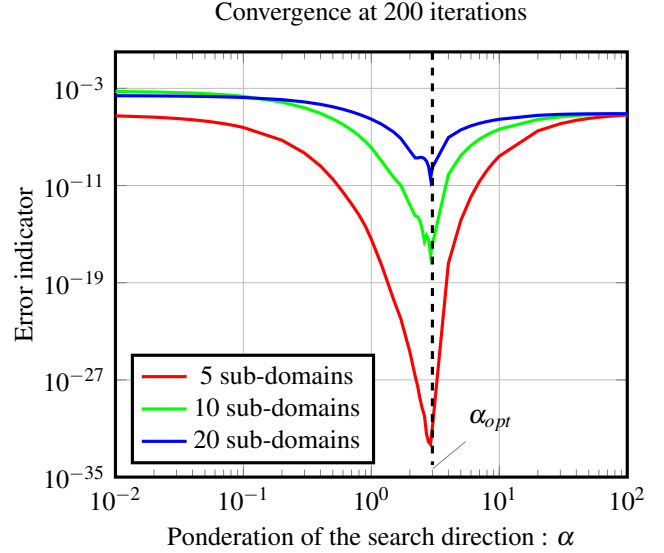


Figure 6: Parametric study of the search direction

condition of unilateral contact with an initial gap j . The structure is under loads F_1 and F_2 defined by two time step t_0 and t_1 . Firstly the structure is pre-load with the load F_1 before loading with F_2 . The materials are still linear elastic defined by the Young modulus E and the Poisson ratio ν . Each sub-structure is discretized by 25×25 elements. The values of the different parameters are in Table 2.

Table 2: Parameters

Parameters	Value/Range
E	210 GPa
h	50 mm
j	0.04 mm
F_1^{max}	50 MPa
F_2^{max}	30 MPa
μ_1	$\in [0, 0.6]$
μ_2	$\in [0, 0.6]$

Depending of the chosen parameters for the Coulomb coefficient, the sub-domain 2 touches or not the boundary condition with the initial gap. So in order to illustrate this behavior, the force reaction on the boundary condition is computed at convergence of the algorithm and plotted depending on the two parameters μ_1 and μ_2 (Figure 8).

Our results correspond to those of Champany and Boucard in [6]. We obtain the different configurations in which the contact on the interface with gap is reached or not. On Figures 9a,9b,9c contact is reached, Coulomb coefficients are too weak to retain the sub-domain 2. On the other hand, on Figure 9d, no contact is obtained on the interface with gap.

This 2D computation of frictional contact validated our non-invasive implementation. The contact formulation imposes to modify the non-local search direction into a local one. The convergence of the algorithm by using the diagonal of the stiffness of the soles as a local search direction proves that the condition of $\mathbf{k}_V^+ = \mathbf{k}_V^-$ is not really necessary.

5.3 A 3D contact problem

A 3D contact problem of a bolted assembly is presented here (Figure 10). The purpose of this example is to show that the non-invasive permits to tackle complex 3D case with frictional contact. The assembly is composed with two plates and three bolts, symmetry is exploited to limit the size of the problem. Each plate is assigned to three

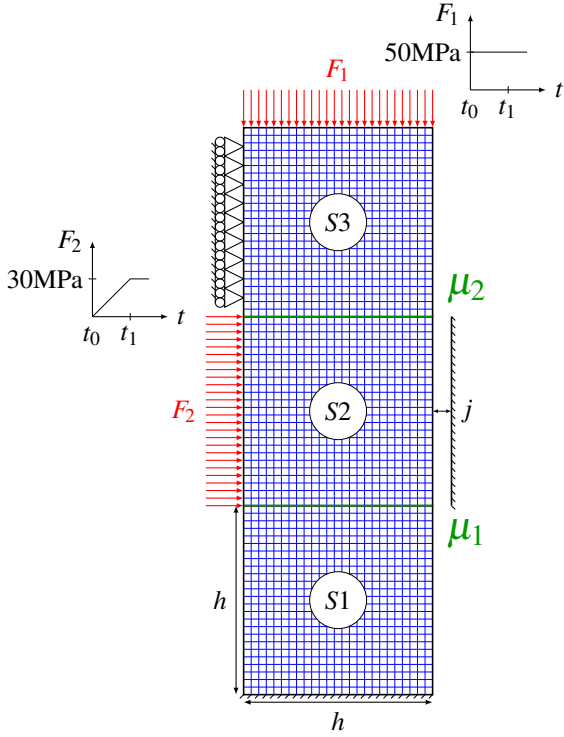


Figure 7: Test case for frictional contact

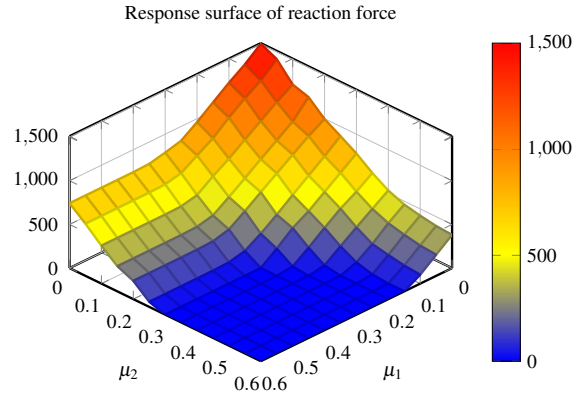


Figure 8: Response surface of the reaction force wrt (μ_1, μ_2)

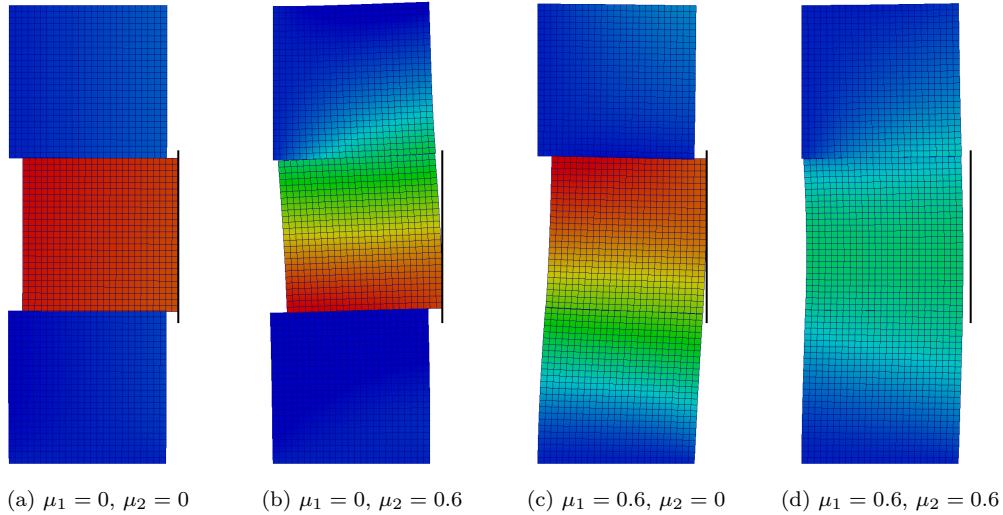


Figure 9: Deformed shape after the second time step for different cases of friction coefficients - Color corresponds to horizontal displacement.

sub-domains. The bolts are also sub-structured in three sub-domains. One is the nut whereas the two others compose the screw. The interface between the two sub-domains of the screw permits to impose a pre-load.

The Young modulus is $E = 200$ GPa, the Poisson's ratio is $\nu = 0.3$. The frictional interface has a Coulomb coefficient of $\mu = 0.1$ and the gap between the screw and the plate is 0.001 mm. These parameters are recalled in Table 3. The problem is computed in four time steps: the first corresponds to the pre-load of the structure, the other ones represent a linear traction force F of the upper plate (Figure 11). The lower plate is fixed on the other side of the assembly.

Remarks: The pre-load is managed with a contact interface. An initial negative gap imposed at the time step t_1 : $\mathbf{B}_n \mathbf{W}|_{t=t_1} = -\mathbf{j}_n$ with $\mathbf{j}_n > 0$ which results in a tension stress in the screw.

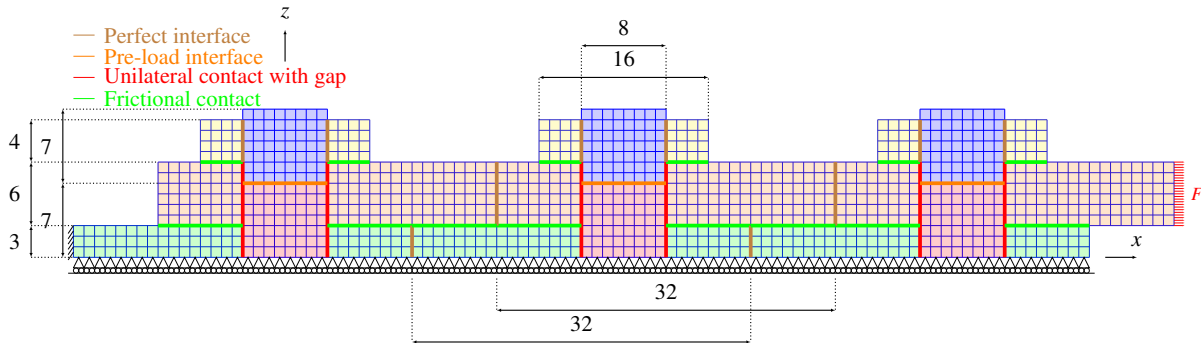


Figure 10: Description of the interfaces and boundary conditions

Table 3: Parameters

Parameters	Value/Range
E	200 GPa
ν	0.3
pre-load j	0.001 mm
Time step	1 s
Number timestep	4
F_{max}	30 MPa
μ	0.1
gap j_n	0.001
Size mesh h	0.5 mm

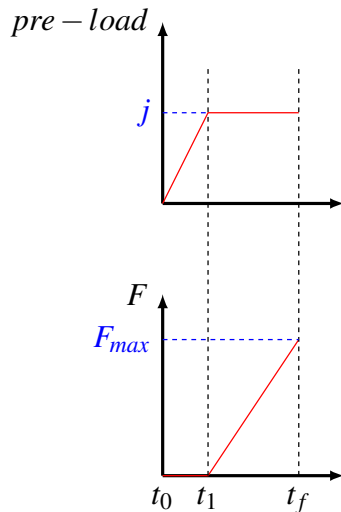


Figure 11: History of the pre-loads in screws and load F

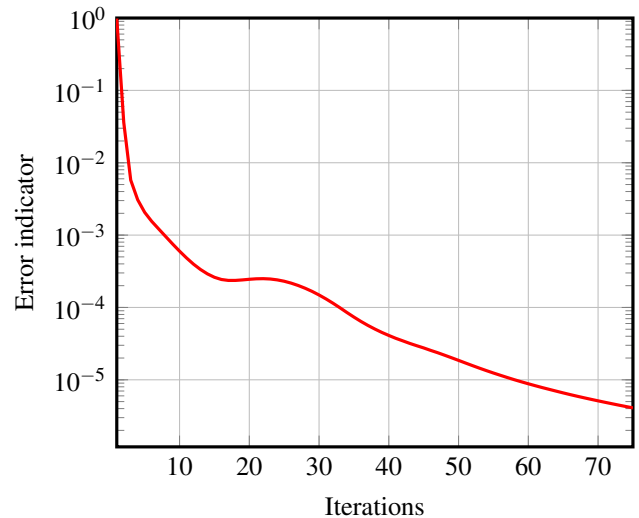


Figure 12: Error indicator

On Figure 13a we represent the elements in compression (σ_{zz} is negative) when the pre-load is imposed. On this example we find the classical Röttscher's pressure cone under the head of the screw [28] and the tension in the body of the screw on Figure 13b. The shearing stress σ_{xz} at the last time step is shown on Figure 14a. Stresses concentrate under heads of screws, due to relative movements of plates. The different contact zones are represented

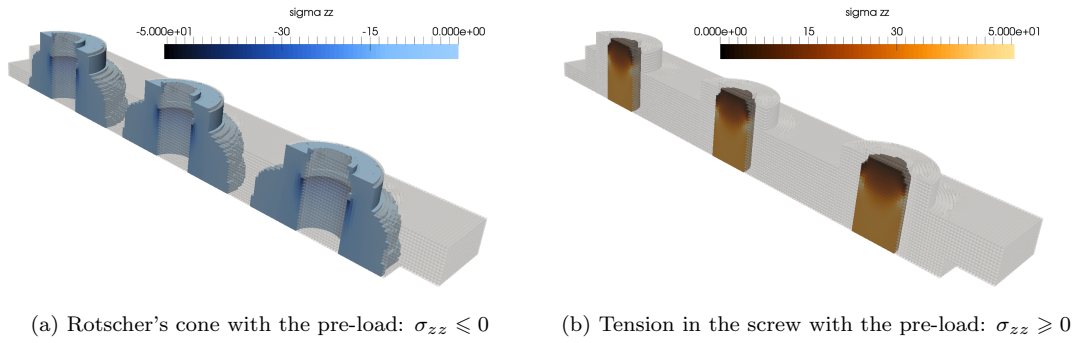


Figure 13: Stress in MPa at the time step t_1

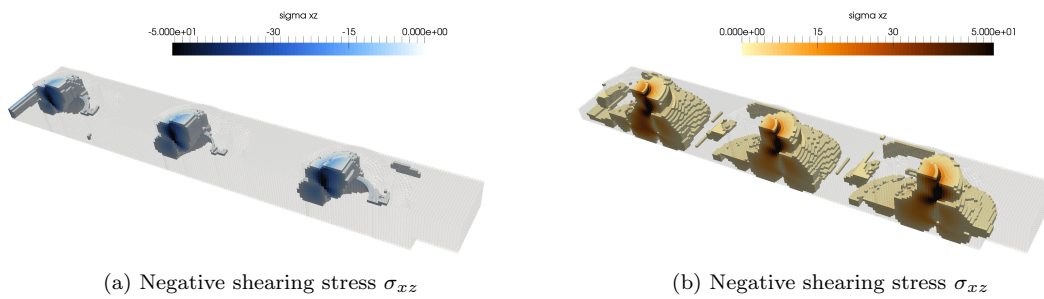


Figure 14: Stress in MPa at the last time step t_f

in black on Figure 15 and a detachment of the two plates is visible between the screws. The error indicator is presented on Figure 12.

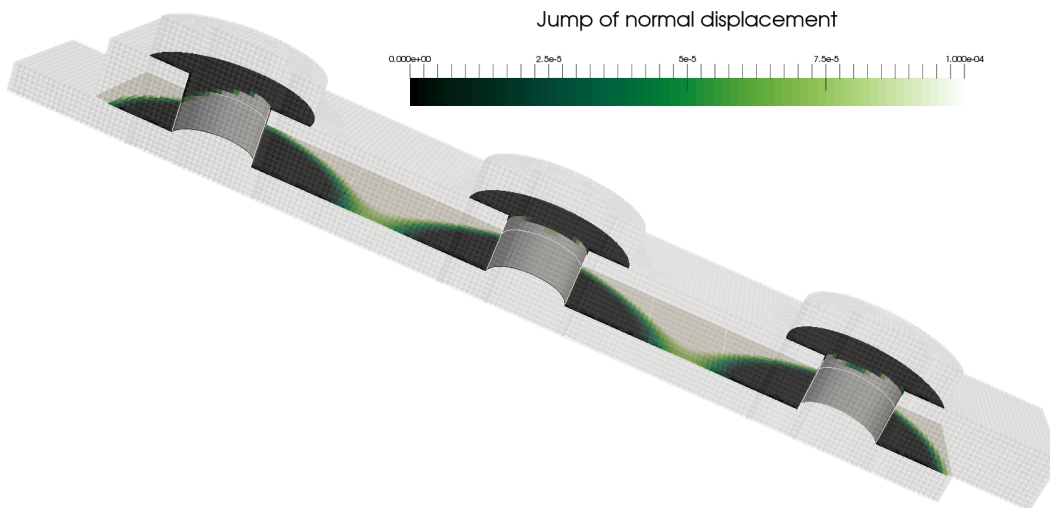


Figure 15: Contact zones in black - jump of displacement in mm

This last use-case was derived from actual engineering activities experienced at Airbus. It highlights how the non-invasive methods permits to overcome critical issues raised by such configurations (multi bolts joints with significant structural effects of friction and pre-loads). These issues still prevent today from proper computations with commercial software, and demand expensive and time consuming experimental protocols when certifying.

A main appeal of non-invasive methods for industry is to allow accurate computational investigations (rather than tests), while skipping any refurbishment of existing numerical frameworks: as demonstrated, non-invasive capabilities can be embedded in day-to-day commercial FE software.

6 Conclusion

In this paper we have presented a non-invasive derivation of a mixed domain decomposition capable of dealing with frictional contact interfaces. In particular the linear stage of the Latin method has been modified to handle Robin conditions over the boundaries of the sub-domains. A non-local stiffness operator has been proposed to compute the search direction on the interfaces. It transforms the standard formulation into a simple assembly of stiffness over the sub-domains that any commercial software is able to compute.

The implementation of this derivation has been validated on a simple test case. Classical results of the Latin method about the influence of the search direction can be applied to our new non-invasive method: the optimal search direction does not depend on the sub-structuring but on the global structure.

The contact formulation imposes a scalar node-wise search direction at the local stage that implies different up and down search direction ($\mathbf{k}_{\bar{v}} \neq \mathbf{k}_{\bar{v}}^{\dagger}$). In order to avoid convergence problems we need to have the closest local search direction from the non-local one. In that sense we choose the scalar search direction as the diagonal of the stiffness operator of the sole. According to that operation we transform the non-local behavior of the interfaces into a decoupled behavior suited to contact formulation. Numerical examples on a 2D academic case confirm the convergence of the algorithm and a first 3D contact problem of a bolted assembly has been presented

The future works will consist in implementing the extensibility of the method. This multi-scale approach, in the mean of [26], modifies the linear stage by introducing a macro resolution that ensures a global equilibrium of force distributions. This approach will be seen as a particular choice of the search direction that makes appear a specific macro projector. The multi-scale extensibility will be coupled with a parallel implementation of the algorithm in order to investigate its scalability.

Acknowledgements

We thank Airbus Group Innovations and EDF for their financial and technical support.

References

- [1] P. Alart and A. Curnier. A mixed formulation for frictional contact problems prone to Newton like solution methods. *Computer Methods in Applied Mechanics and Engineering*, 92(3):353–375, 1991.
- [2] F. Belgacem, P. Hild, and P. Laborde. Recent Advances in Contact Mechanics The mortar finite element method for contact problems. *Mathematical and Computer Modelling*, 28(4):263–271, 1998.
- [3] F. Ben Belgacem and Y. Maday. The mortar element method for three dimensional finite elements. *ESAIM: Mathematical Modelling and Numerical Analysis*, 31(2):289–302, 1997.
- [4] X.-C. Cai, C. Farhat, and M. Sarkis. A minimum overlap restricted additive schwarz preconditioner and applications to 3d flow simulations. *Contemporary Mathematics*, 218:479–485, 1998.
- [5] X.-C. Cai and M. Sarkis. A restricted additive schwarz preconditioner for general sparse linear systems. *Siam journal on scientific computing*, 21(2):792–797, 1999.
- [6] L. Champaney and P. Boucard. Multiresolution strategy for the parametric study of assemblies including contact with friction. In *7th International Conference on Computational Plasticity (COMPLAS), Barcelone, Espagne (cf. p. 41)*, 2003.
- [7] G. Desmeure, C. Rey, P. Gosselet, and P. Cresta. On the representation of interface traction field in a mixed domain decomposition method for structural assemblies. In *WCCM - 10th World congress on computational mechanics*, Sao Paulo, Brazil, 2012.

- [8] C. Dohrmann. A preconditioner for substructuring based on constrained energy minimization. *SIAM Journal on Scientific Computing*, 25(1):246–258, 2003.
- [9] Z. Dostál and D. Horák. Scalable FETI with optimal dual penalty for a variational inequality. *Numerical linear algebra with applications*, 11(56):455–472, jun 2004.
- [10] Z. Dostál, D. Horák, R. Kučera, V. Vondrák, J. Haslinger, J. Dobiáš, and S. Pták. FETI based algorithms for contact problems: scalability, large displacements and 3D Coulomb friction. *Computer Methods in Applied Mechanics and Engineering*, 194(2-5):395–409, feb 2005.
- [11] Z. Dostál, T. Kozubek, T. Brzobohaty, A. Markopoulos, and O. Vlach. Scalable TFETI with optional preconditioning by conjugate projector for transient frictionless contact problems of elasticity. *Computer Methods in Applied Mechanics and Engineering*, 247-248:37–50, nov 2012.
- [12] Z. Dostál, T. Kozubek, V. Vondr, T. Brzobohaty, and A. Markopoulos. Scalable TFETI algorithm for the solution of multibody contact problems of elasticity. *International Journal for Numerical Methods in Engineering*, 82(11):1384–1405, 2010.
- [13] C. Farhat, M. Lesoinne, L. Patrick, K. Pierson, and D. Rixen. FETI-DP: a dual-primal unified FETI method—part I: A faster alternative to the two-level FETI method. *International Journal for Numerical Methods in Engineering*, 50(7):1523–1544, 2001.
- [14] C. Farhat and J. Mandel. The two-level FETI method for static and dynamic plate problems Part I: An optimal iterative solver for biharmonic systems. *Computer Methods in Applied Mechanics and Engineering*, 155(1-2):129–151, mar 1998.
- [15] C. Farhat, J. Mandel, and F. Roux. Optimal convergence properties of the FETI domain decomposition method. *Computer Methods in Applied Mechanics and Engineering*, 115(3-4):365–385, 1994.
- [16] C. Farhat and F.-X. Roux. A method of finite element tearing and interconnecting and its parallel solution algorithm. *International Journal for Numerical Methods in Engineering*, 32(6):1205–1227, 1991.
- [17] M. J. Gander. Optimized Schwarz Methods. *SIAM Review*, 44(2):699–731, 2006.
- [18] R. Glowinski. *Variational Methods for the Numerical Solution of Nonlinear Elliptic Problems*. Society for Industrial and Applied Mathematics, Philadelphia, PA, 2015.
- [19] R. Glowinski and P. Le Tallec. *Augmented Lagrangian and operator-splitting methods in nonlinear mechanics*. SIAM studies in applied mathematics. Society for Industrial and Applied Mathematics, Philadelphia, 1989.
- [20] P. Gosselet and C. Rey. Non-overlapping domain decomposition methods in structural mechanics. *Archives of computational methods in engineering*, 13(4):515–572, 2007.
- [21] P. Gosselet, D. Rixen, F.-X. Roux, and N. Spillane. Simultaneous-FETI and Block-FETI: robust domain decomposition with multiple search directions. *International Journal for Numerical Methods in Engineering*, 104(10):905–927, 2015.
- [22] T. P. Hoang, C. Japhet, M. Kern, and J. Roberts. Ventcell conditions with mixed formulations for flow in porous media. In T. Dickopf, M. Gander, L. Halpern, R. Krause, and L. Pavarino, editors, *Domain Decomposition Methods in Science and Engineering XXII*, pages 531–540, Lugano (Switzerland), 2014.
- [23] P. Kerfriden, O. Allix, and P. Gosselet. A three-scale domain decomposition method for the 3D analysis of debonding in laminates. *Computational Mechanics*, 44(3):343–362, 2009.
- [24] J. Koko. Uzawa block relaxation method for the unilateral contact problem. *Journal of Computational and Applied Mathematics*, 235(8):2343–2356, feb 2011.
- [25] P. Ladevèze. *Nonlinear computational structural mechanics: new approaches and non-incremental methods of calculation*. Mechanical Engineering Series. Springer-Verlag, New-York, 1999.
- [26] P. Ladevèze and A. Nouy. On a multiscale computational strategy with time and space homogenization for structural mechanics. *Computer Methods in Applied Mechanics and Engineering*, 192(28-30):3061–3087, jul 2003.

- [27] J. Mandel and M. Brezina. Balancing domain decomposition: Theory and performance in two and three dimensions. Technical report, University of Colorado at Denver, Denver, CO, USA, 1993.
- [28] F. Rotscher. *Die Maschinenelemente*. Springer-Verlag, Berlin, Germany, 1927.
- [29] K. Saavedra, O. Allix, and P. Gosselet. On a multiscale strategy and its optimization for the simulation of combined delamination and buckling. *International Journal for Numerical Methods in Engineering*, 91(7):772–798, 2012.
- [30] K. Saavedra Redlich. *Stratégie multiéchelle pour l'analyse du couplage flambage-délamination de composites stratifiés*. PhD thesis, École normale supérieure de Cachan, 2012.
- [31] J. C. Simo and T. Laursen. An augmented Lagrangian treatment of contact problems involving friction. *Computers & Structures*, 42(1):97–116, 1992.
- [32] J. C. Simo, P. Wriggers, and R. L. Taylor. A perturbed Lagrangian formulation for the finite element solution of contact problems. *Computer Methods in Applied Mechanics and Engineering*, 50(2):163–180, aug 1985.
- [33] N. Spillane and D. J. Rixen. Automatic spectral coarse spaces for robust FETI and BDD algorithms. *Internat. J. Num. Meth. Engin.*, 95(11):953–990, 2013.
- [34] P. Wriggers. Finite element methods for contact problems with friction. *Tribology International*, 29(8):651–658, dec 1996.
- [35] V. A. Yastrebov. *Numerical Methods in Contact Mechanics*. Numerical methods in engineering series. ISTE/Wiley, London (UK) / Hoboken NJ (US), 2013.